Grain-scale processes in actively deforming magma mushes: New insights from electron backscatter diffraction (EBSD) analysis of biotite schlieren in the Jizera granite, Bohemian Massif

Jiří Žák [a,b,*], Kryštof Verner [b,c], Patricie Týcová [d]

[a] Institute of Geology and Paleontology, Faculty of Science, Charles University, Albertov 6, Prague, 12843, Czech Republic
[b] Czech Geological Survey, Klárov 3, Prague, 11821, Czech Republic
[c] Institute of Petrology and Structural Geology, Faculty of Science, Charles University, Albertov 6, Prague, 12843, Czech Republic
[d] Czech Geological Survey, Geologická 6, Prague, 15200, Czech Republic

ARTICLE INFO

ABSTRACT

In the porphyritic Jizera granite, Bohemian Massif, three distinct types of lattice-preferred orientations of biotite grains were revealed in schlieren-delineated magmatic structures using the electron backscatter diffraction (EBSD) method. (1) Biotite basal planes (001) reorient from schlieren-subparallel near the schlieren base to schlieren-perpendicular in the upper part of the schlieren. Both orientations share subhorizontal ~N–S to ~NNE–SSW-trending a axes. (2) In some domains, the a axes are steep and at a high angle to the schlieren plane while the c axes plunge shallowly and rotate around an ill-defined a axis. (3) In other domains, the EBSD coincides with background magnetic fabric of the host granite revealed using the anisotropy of magnetic susceptibility (AMS) method: that is, the a axes plunge shallowly to the SE or NW while the c axes are subhorizontal and cluster around the ~NE–SW trend.

These multiple biotite orientations in the schlieren are interpreted to reflect (1) velocity-gradient in laminar magma flow along channel-like conduits, localized within the high-strength host phenocryst framework, (2) grain-scale gravity-driven constrictional deformation of the magma mush, and (3) overprinting background (tectonic?) deformation transmitted across large parts of the magma chamber prior to its final crystallization. The grain-scale mechanisms of biotite fabric acquisition in the schlieren presumably involved rotation of biotite crystals during flow, with the biotite alignment reflecting the flow geometry and kinematics, replaced after flow cessation by melt-aided grain-boundary sliding of those biotite crystals still enclosed in melt pockets within otherwise static, highly crystallized magma mush. The latter process was sufficient to reorient biotite grains but not to cause destruction of the schlieren.

Using the Jizera granite as a case example, we argue that the lattice-preferred orientation of mineral grains in mafic schlieren is highly sensitive to reorient in response to processes both associated with the schlieren formation (e.g., localized magma flow) and those that occur later and are superimposed onto the effectively solid, high-strength magma mush.

© 2008 Elsevier B.V. All rights reserved.

1. Introduction

Mafic schlieren are variously-shaped modal concentrations of mafic minerals that occur as small-scale structures in granitoid plutons and diatexites. In many cases, schlieren have one sharp contact against the host rock while the other margin is gradational (e.g., Weinberg et al., 2001; Milord and Sawyer, 2003). Despite their negligible size with respect to the host plutons, schlieren are important markers of the rheological state of the magma and of a wide variety of physical processes in magma chambers, such as convection, magma flow, or gravitational differentiation (e.g., Cloos, 1925; Barriére, 1981; Clarke and Clarke, 1998; Weinberg et al., 2001; Milord and Sawyer, 2003; Pons et al., 2006; Wiebe et al., 2007; Barbey et al., 2008).

Unlike most studies, which have dealt with mafic schlieren in terms of their field relationships, overall geometry, or chemical composition, we focus here on their internal fabric, i.e., the preferred orientation of mafic minerals inside the schlieren. In an attempt to understand the grain-scale processes and hypersolidus finite strain recorded by schlieren, the electron backscatter diffraction (EBSD) method was employed to analyze the lattice-preferred orientation of biotite in variously-shaped schlieren in the porphyritic Jizera granite of the Krkonoše–Jizera Plutonic Complex, Bohemian Massif. This granite is unusual in that it hosts some complex schlieren-bounded

* Corresponding author. Institute of Geology and Paleontology, Faculty of Science, Charles University, Albertov 6, Prague, 12843, Czech Republic.
E-mail address: jirizak@natur.cuni.cz (J. Žák).
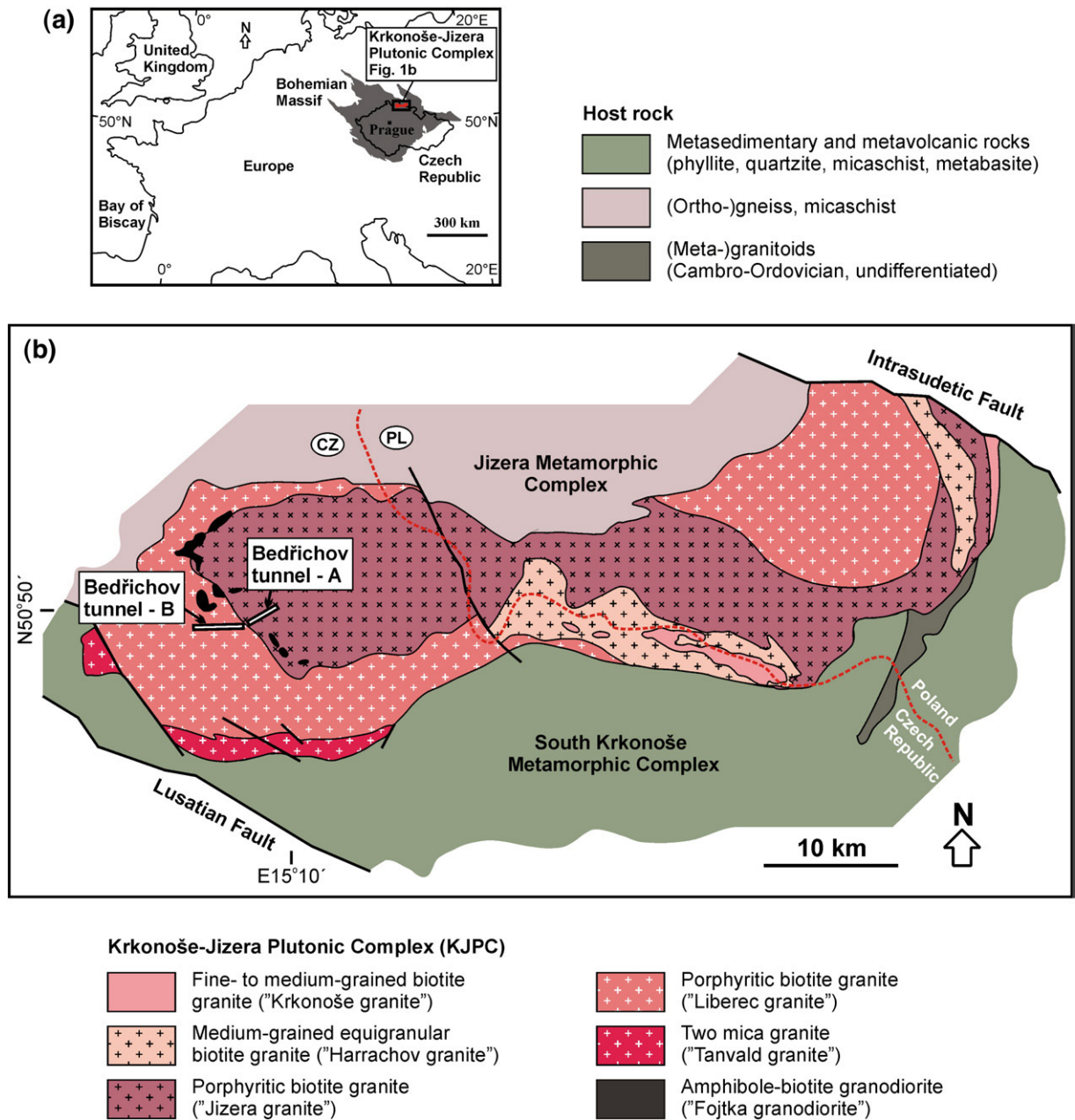
Fig. 1. (a) Index map showing the location of the Krkonoše–Jizera Plutonic Complex in the northeastern part of the Bohemian Massif, central Europe. (b) Simplified bedrock geologic map of the Krkonoše–Jizera Plutonic Complex and its host rock. The Bedřichov tunnel A is located in the porphyritic Jizera granite near its southwestern margin. Geology compiled from Klomínský (2005) and Kozdrój et al. (2001).

magmatic structures (troughs, tubes, ladder dikes, magmatic folds) described in detail in our previous work (Žák and Klomínský, 2007).

The advantages of examining the crystallographic preferred orientation of component mineral grains in schlieren are twofold. First, compared to "conventional" image analysis of shape-preferred orientation of mineral grains, for instance from thin-sections, the EBSD method yields precise orientations of all crystallographic axes in three dimensions. Second, the lattice-preferred orientation is less sensitive to modification by late postcumulus processes, such as contact melting or textural maturation (e.g., Park and Means, 1996; Holness, 2007), which may alter the original grain shape and thus the shape-preferred orientation acquired during the schlieren formation.

The key issue we wish to address is to what extent the lattice-preferred orientation of biotite in schlieren can record successive strain increments resulting both from localized magma flow during schlieren formation and from large-scale deformation of the host magma mush in a crystallizing

chamber. We first briefly describe the geological setting of our study area, the background magnetic (AMS) fabric of the host Jizera granite, the geometry of schlieren-bounded magmatic structures, and the results of our EBSD analysis of biotite in the schlieren. We then discuss the possible geometrical characteristics of the internal fabric in mafic schlieren to develop some testable criteria for the interpretation of the mechanical processes and strain recorded by mineral fabric inside the schlieren. Finally, on the basis of comparison of AMS and EBSD data, we interpret the processes that may have operated in a crystal-rich magma mush at the grain-scale during and after schlieren formation.

2. Geological setting

The ~ 1000 km^2 Carboniferous Krkonoše–Jizera Plutonic Complex (also variously referred to as the Krkonoše–Jizera pluton or massif in the Czech literature, Riesengebirge in German, or the Karkonosze
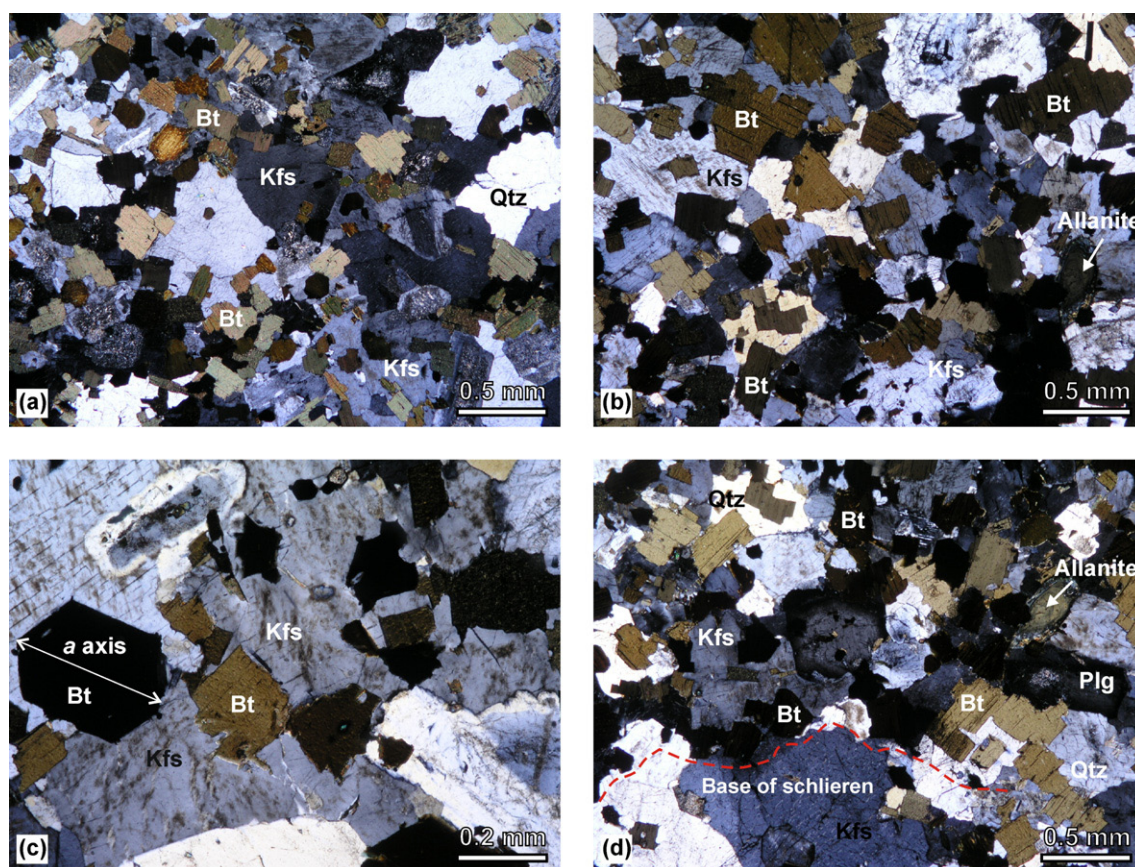
Fig. 2. Magmatic microstructures of biotite schlieren in the Jizera granite. (a) Central part of schlieren, sample BTS3. (b) Central part of schlieren, sample BTS4. (c) Close-up of biotite grains overgrown by K-feldspar. Note that the *a* axis of the euhedral biotite crystal is longer than the *b* axis (thin-section is parallel to its basal plane); sample BTS2. (d) Base of schlieren, sample BTS4. Crossed nicols. Mineral abbreviations: Bt — biotite, Kfs — K-feldspar, Plg — plagioclase, Qtz — quartz.

pluton in Polish) in the northern part of the Bohemian Massif (Fig. 1a, b) has been a classic area of granite geology since the pioneering work of Cloos (1925). In map view, the plutonic complex has a "double lobed" shape with a narrow central part and its longest dimension (~70 km) elongated ~E–W. The plutonic complex intruded several lithotectonic units of Neoproterozoic to Paleozoic age, which have been interpreted as tectonostratigraphic terranes with contrasting histories separated by major faults and shear zones (for reviews and further information see, e.g., Cymerman et al., 1997; Zelazniewicz, 1997; Aleksandrowski et al., 1997, 2000; Mazur and Aleksandrowski, 2001; Aleksandrowski and Mazur, 2002; Marheine et al., 2002; Mazur, 2002; Hladil et al., 2003; Winchester et al., 2003; Mazur et al., 2006).

The plutonic complex is a composite body and comprises several lithologic units (Fig. 1b; Borkowska, 1966; Klomínský, 1969; Słaby and Götze, 2004; Słaby et al., 2002, 2007a,b; Słaby and Martin, 2008). The southwestern margin of the complex is made up of two-mica granite, while much of the remainder of the plutonic complex consists of two varieties of coarse-grained porphyritic biotite granodiorite to granite (the Jizera and Liberec granites in Fig. 1b). The gradational internal contact between the porphyritic granites is delineated in places by smaller bodies of more mafic, amphibole–biotite granodiorite (Fig. 1b). Medium-grained biotite granite crops out in two isolated bodies in the eastern half of the plutonic complex. The uppermost exposed part of the plutonic complex is made up of fine- to medium-grained equigranular biotite granite (Fig. 1b). The granitoids are also cross-cut by comagmatic aplite dikes and late lamprophyre dikes of uncertain origin (Słaby and Martin, 2008).

The existing radiometric ages of the units range widely from 329± 17 Ma (porphyritic granite; Rb–Sr whole rock; Duthou et al., 1991) to 304±14 Ma (the Liberec granite; Pb–Pb on zircon; Kröner et al., 1994).

The most recent SHRIMP dating yielded zircon ages ~318–314 Ma for the porphyritic and equigranular granites, respectively (Machowiak and Armstrong, 2007).

This study examines mafic schlieren superbly exposed in the Bedřichov tunnel A (Fig. 1b), which cuts through the porphyritic biotite granite (the Jizera granite) in the western part of the plutonic complex. Importantly, no evidence of solid-state flow or recrystallization (using the criteria of Paterson et al., 1989 and Vernon, 2000) exists either in the host granite or the schlieren. The textures are exclusively magmatic, characterized by euhedral to subhedral mineral grains (Fig. 2). The Jizera granite is predominantly composed of subhedral crystals of K-feldspar, plagioclase, quartz, and biotite, and the schlieren are defined by modal concentration of biotite. Biotite grains in the schlieren do not contain mineral inclusions and are commonly enclosed in quartz and K-feldspar aggregates (Fig. 2b, d). Large biotite grains (more than ~0.3 mm in size) are subhedral to irregular with well developed cleavage (Fig. 2b, upper left), whereas small biotite grains (less than ~0.3 mm in size) are euhedral (Fig. 2c). It is important to note that the euhedral biotite crystals are not perfectly hexagonal in thin-section, but instead have the *a* axis longer than the *b* axis (e.g., Fig. 2c). The schlieren microstructure resembles poikilitic texture common in mafic magmatic rocks (e.g., Mitchell et al., 1998) and thus may reflect rapid overgrowth of biotite crystals by the K-feldspar and quartz aggregates from late interstitial melt.

3. Background magnetic fabric of the host Jizera granite

Before examining the centimeter-scale biotite fabric variations in mafic schlieren, we describe magmatic (magnetic) fabric of the Jizera granite to provide information on the background fabric away from
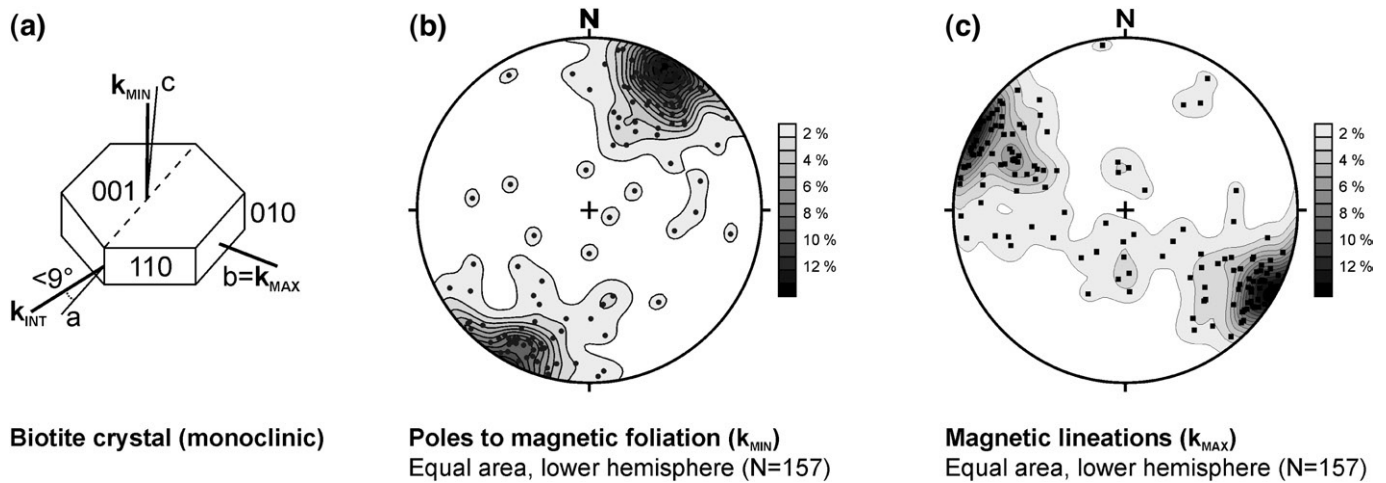
Fig. 3. (a) Orientation of principal susceptibilities (k_{MAX} — maximum principal susceptibility, k_{INT} — intermediate principal susceptibility, k_{MIN} — minimum principal susceptibility) with respect to the crystallographic axes (a, b, c) of a single biotite crystal. Redrafted from Borradaile (2003). (b) Stereograms (lower hemisphere, equal area projection) summarizing orientations of magnetic foliation poles and (c) magnetic lineations in all AMS samples of the Jizera granite from the Bedřichov tunnel.

the schlieren-bearing structures. This background fabric was investigated by means of the anisotropy of magnetic susceptibility method (AMS), which has routinely been used to reveal "cryptic" magnetic fabric in granitoids (for reviews and basic principles of the method see, e.g., Hrouda, 1982; Tarling and Hrouda, 1993; Bouchez, 1997).

As the full details of our AMS study are given elsewhere (Žák et al., in press), here we present only data directly relevant to schlieren formation. The AMS data were obtained from 43 oriented samples taken at 16 sampling sites between 120–220 m from the western entrance of the Bedřichov tunnel A, i.e., at various distances from the schlieren-bearing structures. The AMS was measured with the KLY-3S Kappabridge apparatus in the Laboratory of Rock Magnetism at AGICO Ltd., Brno, Czech Republic, and a statistical treatment of the AMS data was carried out using the ANISOFT 42 software (written by M. Chadima and V. Jelínek; www.agico.com).

Measurements of susceptibility variations with temperature have shown that the AMS in the Jizera granite is carried by coaxial contributions of biotite, magnetite, and maghemite (Fig. 9 in Žák et al., in press). Orientations of the maximum and minimum magnetic susceptibilities (k_{MAX} or k_1 and k_{MIN} or k_3, respectively) thus also record the orientation of biotite magnetic axes that are at a small angle (less than 9°) to the crystallographic axes (Fig. 3a; see also Borradaile, 2003, p. 304). The small difference in the orientation of the biotite magnetic and crystallographic axes allows direct comparison of the background AMS fabric in the host granite with the lattice-preferred orientation of biotite in the schlieren as measured using EBSD (this section and Section 4 below).

For the purpose of this paper, the AMS data are represented only by the orientations of the principal susceptibilities, k_{MAX} (magnetic lineation) and k_{MIN} (pole to magnetic foliation), plotted in stereograms in the geographic (in situ) coordinate system (Fig. 3b, c). Magnetic foliations dip moderately to steeply and strike WNW–ESE to NW–SE; only a few samples have other orientations (Fig. 3b). Most of the magnetic lineations plunge shallowly to moderately to the NW or SE, defining two prominent maxima at the periphery of the stereogram in Fig. 3c. A small number of lineations plunge steeply at variable trends and define a girdle-like pattern between the two maxima. The magnetic foliations and lineations are thus remarkably homogeneously oriented along the examined section of the tunnel.

4. Electron backscatter diffraction (EBSD) — methodology

The electron backscatter diffraction (EBSD) method (see Prior et al., 1999 for details) has mainly been applied to study the lattice-pre-

ferred orientation of minerals in naturally deformed tectonites (e.g., Lloyd and Freeman, 1994; Fliervoet et al., 1999; Leiss and Barber, 1999; Heidelbach et al., 2000) compared to only a few recent studies on EBSD in plutonic rocks (Verner et al., 2006; Romeo et al., 2007; Žák et al., 2008; McLaren and Reddy, in press).

In this study, two schlieren-bearing structures (hereinafter referred to as "Structure 1" and "Structure 2") exposed in the Bedřichov tunnel A (Fig. 1b) were selected for the EBSD analysis. The selection was made because these two structures represent the most complex cases from a wide variety of magmatic structures described in the granite (Žák and Klomínský, 2007), thus having a greater potential to record multiple processes. The sampling strategy was to examine the biotite fabric variations in the schlieren at different scales. The samples (thin-sections) were taken in different parts of each schlieren-bearing structure to examine variations across the structure at the meter scale. In each thin-section, the lattice-preferred orientation was then measured in two or three domains at various distance from the schlieren base (defined by a sharp bottom margin or side against the host granite) to reveal fabric variations at the cm scale.

The lattice-preferred orientations of the biotite were measured on the CamScan3200 scanning electron microscope in the laboratories of the Czech Geological Survey, Prague. As this technique records electron backscatter diffraction patterns that originate from an interaction depth of a few tens of nanometers, the thin-section surfaces were manually polished using colloidal silica suspension and carbon-coated to avoid charging effects. The EBSD patterns were recorded using an HKL Technology NordlysII camera system and indexed using the Channel5 software (Schmidt and Olesen, 1989). Pattern acquisition was carried out at 20 kV acceleration voltage, ~5 nA beam current, 33 mm working distance, and 70° sample tilt. The analysis was done in manual mode owing to small differences in diffraction patterns, with each individual grain represented by one orientation measurement. Crystallographic orientation data given by three Euler angles φ_1, Φ, and φ_2 were obtained from interactively indexed EBSD patterns. The recorded data also contain the x, y-coordinates of the measured position, the image quality parameters Band contrast (BC) and Band slope (BS), indicating pattern contrast and sharpness of the diffraction bands, and the Mean angular deviation index (MAD), an indexing reliability parameter with values between 0 and 1. The chemistry and orientation of the grains were controlled using a forescatter detector (FSD) with combination of orientation and chemical contrast. For biotite indexation the crystallographic parameters of Bonlen et al. (1980) were used. The orientations of the a, b, c crystallographic axes of the biotite grains were first obtained in the specimen reference
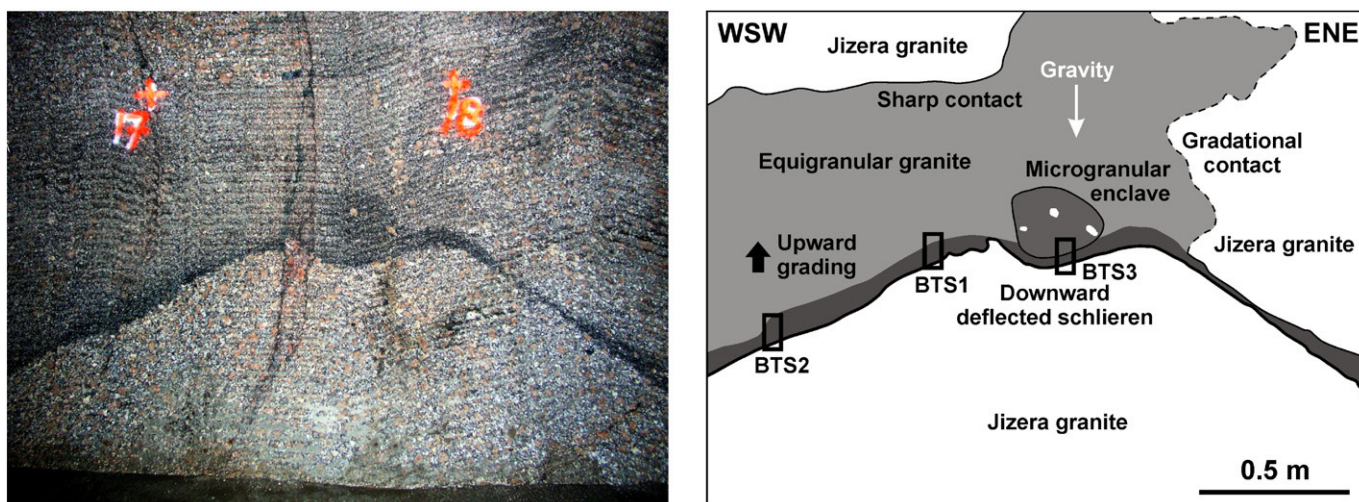
Fig. 4. Schlieren antiform in the Jizera granite, denoted as Structure 1 in this paper. Mafic schlieren in the crestal part of the antiform are deflected downward around a microgranular enclave. Bedřichov tunnel, section A, approximately 336 m from the western entrance. Bold rectangles indicate sample locations.

frame and then rotated into the geographic coordinate system and plotted using the Unicef Careware software written by D. Mainprice (http://www.isteem.univ-montp2.fr/PERSO/mainprice). The crystallographic axes are presented separately in lower hemisphere, equal area projection stereonets.

5. Results

5.1. Structure 1

Structure 1, exposed 336 m from the western entrance of the tunnel, is hosted in the Jizera granite and is defined by upward-grading biotite schlieren having a sharp base. The structure intersects the opposite tunnel walls, establishing its three-dimensional shape and orientation. The overall shape of the structure resembles an antiform (Fig. 4) having a subhorizontal axis trending ~120° (i.e., roughly parallel to the magnetic lineations in the host granite; Fig. 3c). The antiform is overlain by darker, medium-grained, equigranular to weakly porphyritic granite to granodiorite. The contact between the host porphyritic Jizera granite and the darker equigranular granite is mostly sharp but drapes around K-feldspar phenocrysts within the Jizera granite. A microgranular enclave rests on the crestal part of the schlieren antiform (within the darker equigranular granite).

Three samples for the EBSD analysis were taken in different parts of the structure (see Fig. 4 for sample locations); two samples (BTS1 and BTS2) were taken from the limb of the schlieren antiform WSW of the enclave and one sample beneath the enclave (BTS3). Two distinct types of EBSD patterns can be defined in Structure 1 (Figs. 5–7).

(1) The first type is characterized by subhorizontal a axes clustered around a ~N–S to ~NNE–SSW trend and associated with two different distributions of c axes, the latter depending on the distance from the base of the schlieren (Figs. 6a, d, 7d).

Near the sharp base of the schlieren, basal planes (001) of biotite crystals tend to be statistically positioned at a small angle to the base of the schlieren, as documented by the most pronounced maxima of the c axes near the pole to the schlieren in the stereonets (Figs. 6f, 7f). Minor c axes clusters also occur close to the great circle of the schlieren plane in the stereonets (Figs. 6f, 7f), suggesting that some biotite crystals are aligned with their basal planes at a high angle to the schlieren. Moreover, some c axes are scattered in the stereonet in orientations other than those described above.

In the upper part of schlieren, while the a axes retain their ~N–S orientation, the biotite basal planes (001) tend to reorient from

schlieren-parallel (prevailing near the schlieren base) to schlieren-perpendicular. The reorientation of the biotite is indicated by the most prominent c axes maxima positioned on the great circle corresponding to the schlieren plane (Figs. 6c, 7c), and is most clearly shown in Fig. 6c where the subordinate maximum of the c axes plots near the pole to the schlieren plane and passes through a weak girdle to a major maximum within the schlieren plane (represented by great circles in Fig. 6c).

(2) The other type of EBSD pattern is characterized by the a axes forming several component maxima along a ~NW–SE plane (Fig. 7a). The most striking maximum in this case corresponds to the a axes shallowly plunging to the ~NW (Figs. 5g, 7a) while the c axes are predominantly subhorizontal and either trend ~NNE–SSW (two subordinate maxima in Fig. 7c) or plot near the schlieren great circle, corresponding to biotite grains nearly perpendicular to the schlieren (Figs. 5i, 7c).

Unlike the two generally simple patterns described above, sample BTS1 exhibits a more complex orientation distribution of biotite crystallographic axes (Fig. 5). Near the schlieren base, the a axes are subhorizontal and trend ~SE (prominent cluster in Fig. 5g), whereas in the upper part of the schlieren the a axes trend predominantly ~N–S to ~NNE–SSW, similar to samples BTS2 and BTS3 (compare to Figs. 6a, d and 7d). In contrast, the c axes exhibit no simple pattern and are scattered over the stereonets, with multiple strong maxima (Fig. 5c, f, i). Some trends in the c axes orientation distribution across the schlieren can be recognized in spite of the wide scatter. Near the base of the schlieren, the most significant cluster of c axes is around a ~SSE trend, while other subordinate maxima lie along the schlieren great circle or are near the pole to the schlieren (Fig. 5i). The central and upper part of the schlieren are also characterized by a multimodal distribution of c axes orientations, but some of the major clusters are in the proximity of the pole to the schlieren or tend to concentrate along the schlieren great circle (Fig. 5c, f).

5.2. Structure 2

Structure 2, exposed in the Bedřichov tunnel A 210 m from its western entrance, resembles a schlieren anticline (younging upwards as inferred from schlieren truncations) defined by planar, upward-graded schlieren to form fold limbs with cross-cutting schlieren channels preserved in the crestal part of the anticline (Fig. 8). K-feldspar phenocrysts are concentrated above the schlieren of one fold limb, with the schlieren being deflected around the base of the

Sample BTS1 - upper part of schlieren, ~3.3 cm from base

(a) *a* axes   **(b)** *b* axes   **(c)** *c* axes
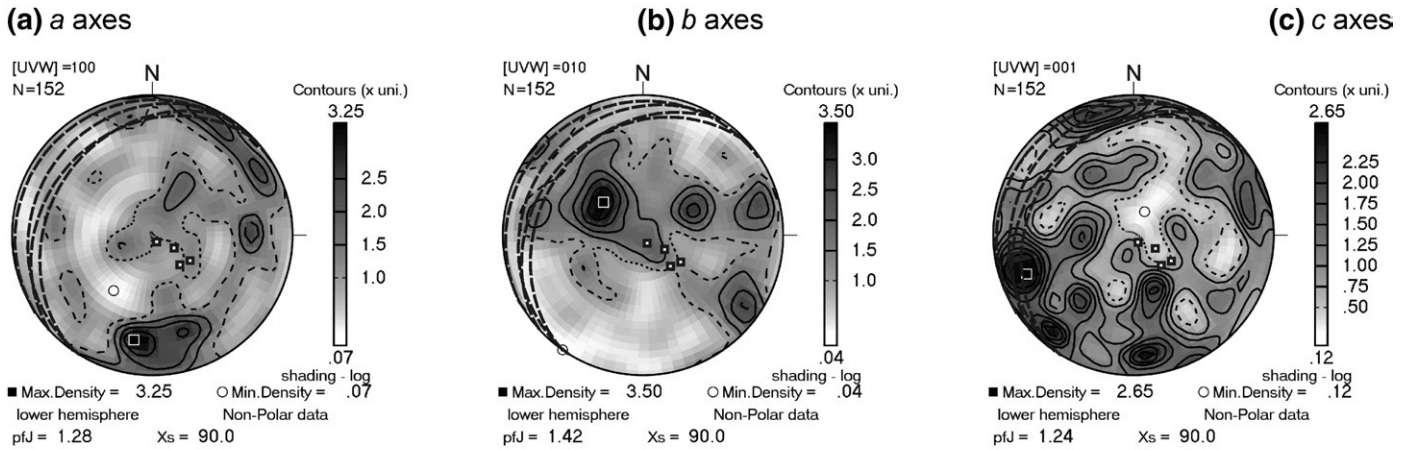
Sample BTS1 - central part of schlieren, ~1.8 cm from base

(d) *a* axes   **(e)** *b* axes   **(f)** *c* axes
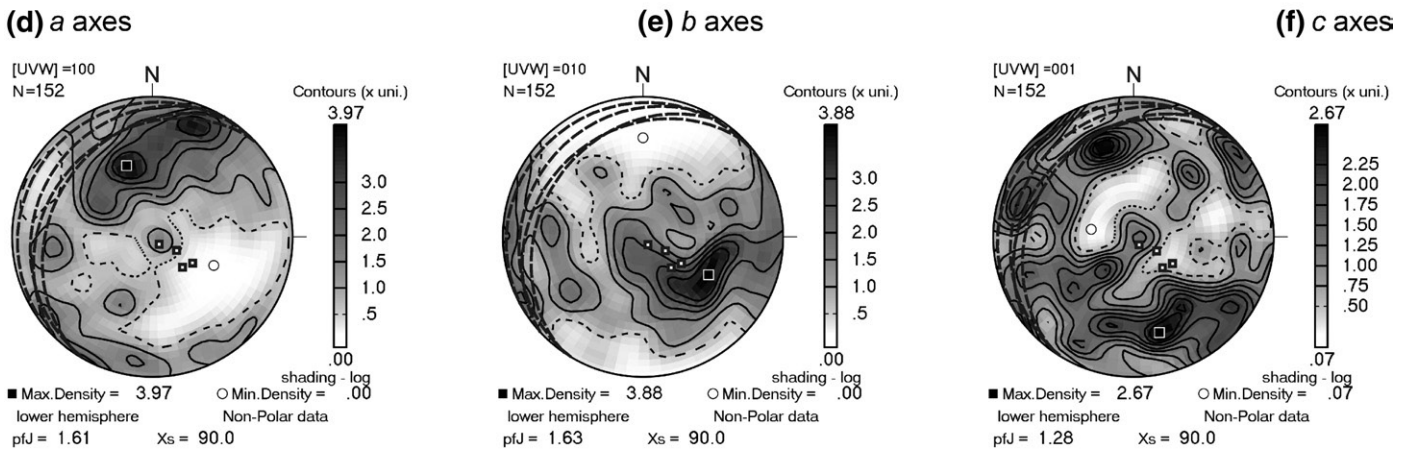
Sample BTS1 - base of schlieren

(g) *a* axes   **(h)** *b* axes   **(i)** *c* axes
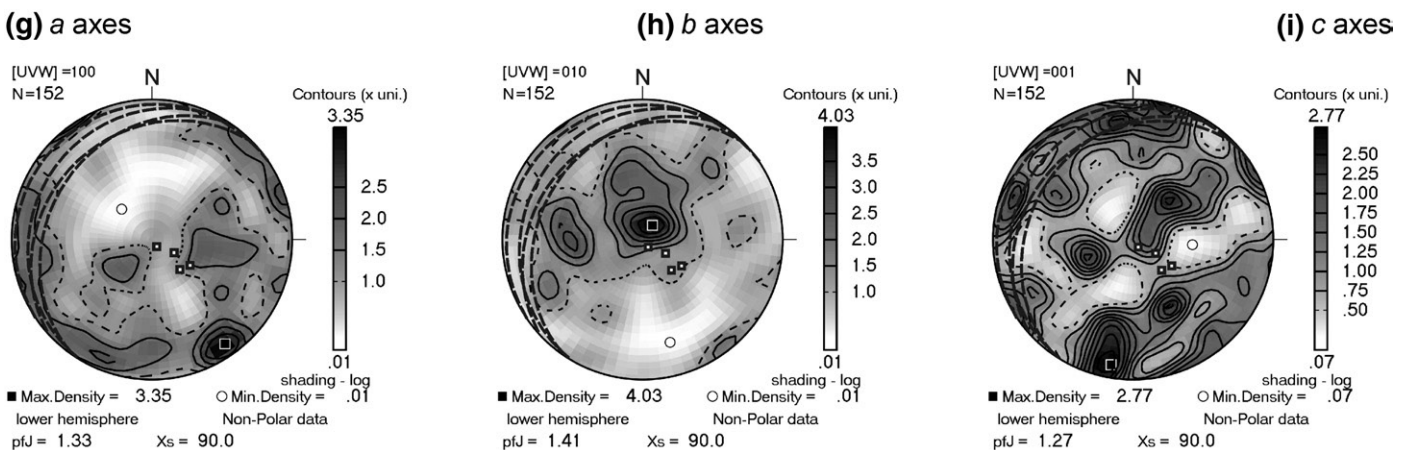
Great circle (dashed) - schlieren plane ▫ Pole to the schlieren plane

Fig. 5. Stereographic projection (equal area, lower hemisphere) of orientations of biotite crystallographic axes (*a, b, c*) in sample BTS1 (Structure 1) obtained using the EBSD method. The analysis was carried out in three domains at various distances from the base of the schlieren. See Fig. 4 for sample location. Orientations are shown in the geographic coordinate system.

accumulation. A large xenolith of coarse-grained porphyritic granite of uncertain origin rests on top and deforms the underlying K-feldspar accumulation. The upper part of this complex structure is formed by a leucocratic (pegmatite, aplite) layer, also being folded roughly parallel to the mafic schlieren. The pegmatite layer is not disrupted by the xenolith, and thus must represent a feature that postdates the xenolith

Sample BTS2 - upper part of schlieren, ~3.7 cm from base

(a) *a* axes **(b)** *b* axes **(c)** *c* axes
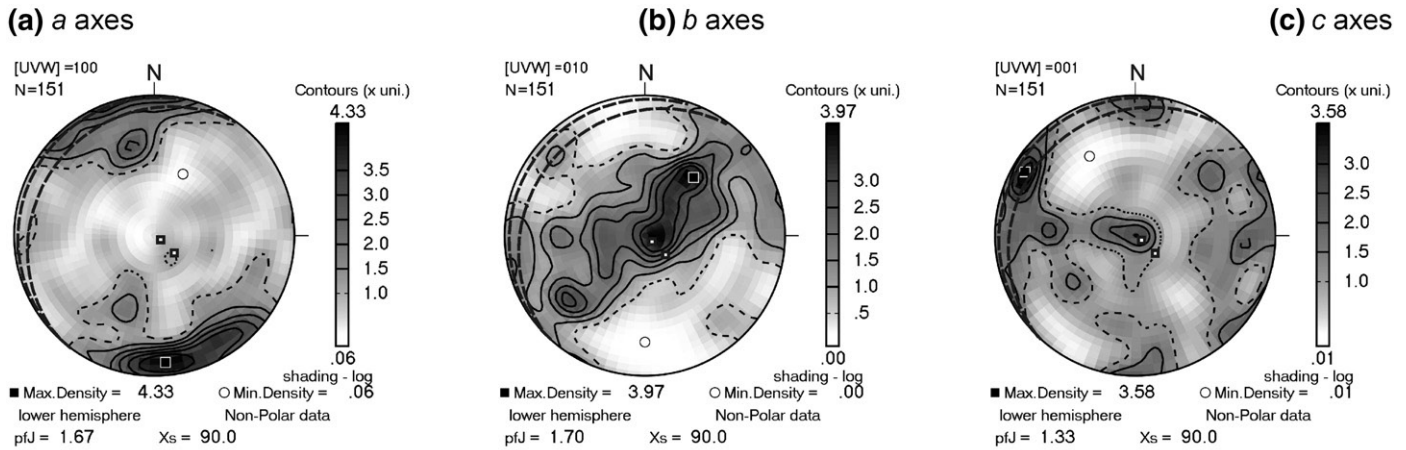
Sample BTS2 - base of schlieren

(d) *a* axes **(e)** *b* axes **(f)** *c* axes
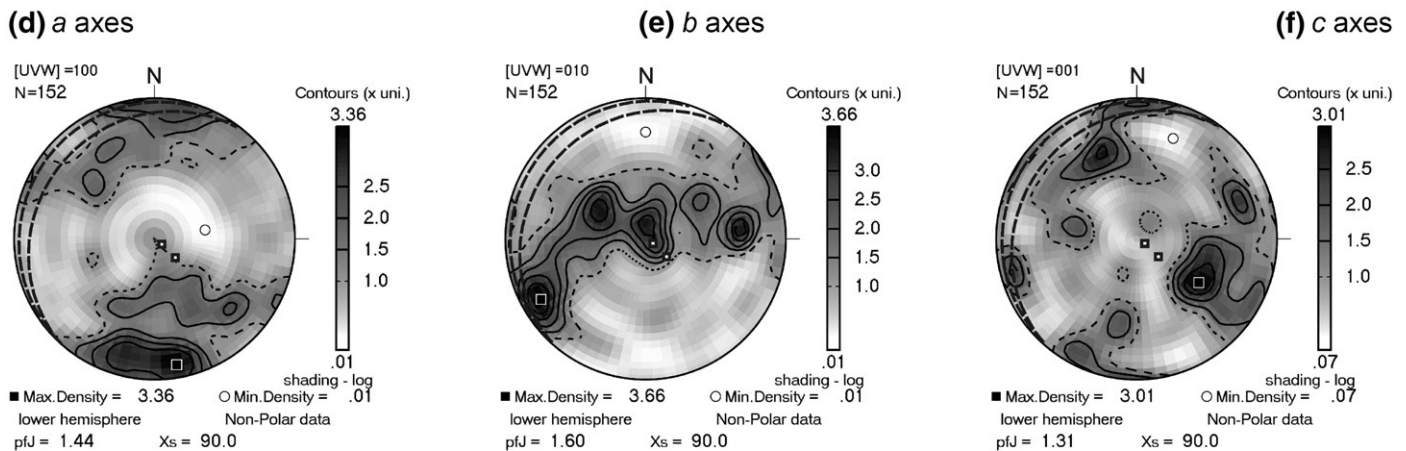
Great circle (dashed) - schlieren plane □ Pole to the schlieren plane

Fig. 6. Stereographic projection (equal area, lower hemisphere) of orientations of biotite crystallographic axes (*a*, *b*, *c*) in sample BTS2 (Structure 1) obtained using the EBSD method. The analysis was carried out in two domains at various distances from the base of the schlieren. See Fig. 4 for sample location. Orientations are shown in the geographic coordinate system.

sinking. The magmatic fold is discordantly truncated by a submagmatic crack with sharp outer margins delineated by mafic schlieren and filled by the "normal" porphyritic Jizera granite.

The samples were taken from the crestal region of the schlieren anticline (sample BTS4) and from its ENE limb where the schlieren are approximately planar (BTS5). In sample BTS4, the *a* axes exhibit remarkably similar orientations, both in the underlying granite and across the schlieren. Most of the *a* axes plunge moderately to steeply, forming a broad cluster with pronounced maxima around the centre of the stereonet (Fig. 9a, d, g). That is, biotite crystals are generally oriented steeply in the gently-dipping schlieren (Fig. 8). Subordinate maxima of the *a* axes also plot close to the schlieren great circle (Fig. 9d). In the upper part of the schlieren, the *a* axes maxima form an ~E–W elongated girdle with two maxima, one near the stereonet center and one at the schlieren great circle (Fig. 9a, d, g). The *b* and *c* axes exhibit a multimodal orientation distribution (Fig. 9b, c, e, f, h, i), but their maxima tend to concentrate around a circle or ellipse positioned symmetrically (Fig. 9c, i) or asymmetrically (Fig. 9f) with respect to the center of the stereonet, suggesting rotation of the two axes around an ill-defined *a* axis. This means that the steeply oriented biotite flakes rotate around a fixed steep *a* axis so as the *b* and *c* axes vary with little preferred orientation of their own.

In sample BTS5, the *a* axes define a girdle oriented at a high angle to the strike of schlieren (i.e., ~NE–SW), regardless of distance from the schlieren base (Fig. 10a, d). Three distinct maxima of the *a* axes occur within the girdles, one near the schlieren plane, one close to the center of the stereonet or close to the schlieren pole, and one gently plunging to the SW (Fig. 10a, d). The *c* axes in the basal part of the schlieren cluster along the periphery of the stereonet (Fig. 10f), whereas in the upper part they reveal a more complex, rather scattered pattern with multiple maxima (Fig. 10c).

6. Discussion

Several processes have been proposed to account for the formation of mafic schlieren in granite plutons or migmatite complexes (e.g., Barriére, 1981; Clarke and Clarke, 1998; Milord and Sawyer, 2003; Weinberg et al., 2001; Pons et al., 2006; Pupier et al., 2008; Barbey et al., 2008): (1) disintegration of microgranular enclaves or xenoliths, (2) preferential crystallization of mafic minerals driven by steep physicochemical gradients along contacts (Naney and Swanson, 1980), (3) multiple magma injections, (4) gravitational settling, (5) velocity-gradient flow sorting, (6) coupled flow sorting and melt extraction

Sample BTS3 - upper part of schlieren, ~3.8 cm from base

(a) *a* axes

(b) *b* axes

(c) *c* axes

Sample BTS3 - base of schlieren

(d) *a* axes

(e) *b* axes

(f) *c* axes

Great circle (dashed) - schlieren plane ▫ Pole to the schlieren plane
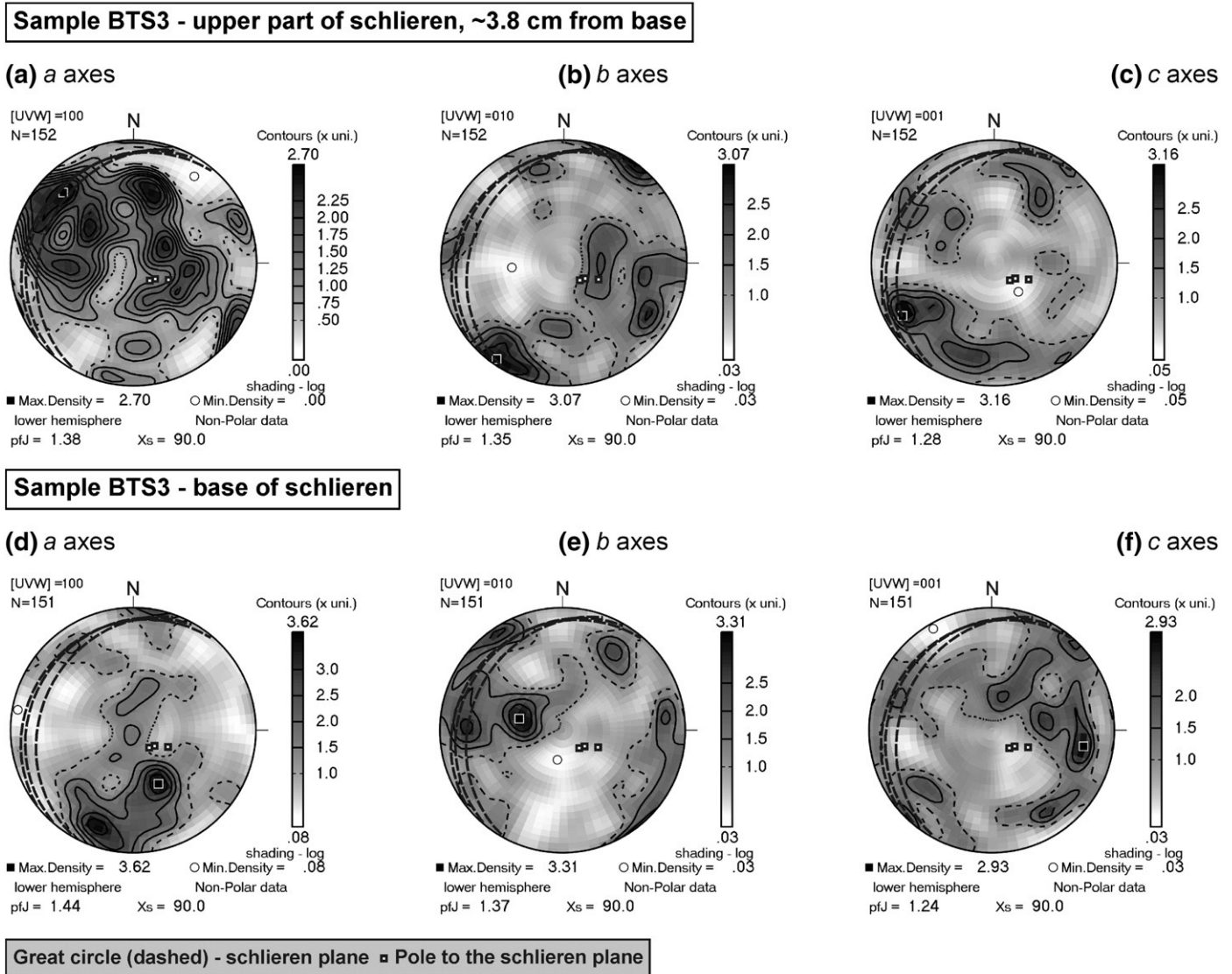
Fig. 7. Stereographic projection (equal area, lower hemisphere) of orientations of biotite crystallographic axes (*a*, *b*, *c*) in sample BTS3 (Structure 1) obtained using the EBSD method. The analysis was carried out in two domains at various distances from the base of schlieren. See Fig. 4 for sample location. Orientations are shown in the geographic coordinate system.

from schlieren into the surrounding porous mush (Weinberg et al., 2001), or (7) flow of magma mush around a sinking enclave (Wiebe et al., 2007). To begin the analysis of the results, we first attempted to outline the expected (ideal) fabric characteristics in relation to some basic mechanical processes of schlieren formation (Fig. 11), excluding hypotheses 1, 2, and 7, which we find unlikely to explain the origin of the schlieren under study (Žák and Klomínský, 2007). For the sake of simplicity, only biotite is considered as the dominant constituent mineral in the schlieren, as it is in the case of the Jizera granite. Despite the great oversimplification, Fig. 11 illustrates that each single process should leave behind distinct characteristics of internal schlieren fabric and thus also a distinct orientation distribution of biotite crystallographic axes. In reality, possible factors which could complicate the simple biotite fabrics shown in Fig. 11 may involve (i) flow and deformation processes leading to complex orientation distribution of mineral grains (e.g., S–C fabrics in simple shear; Blumenfeld and Bouchez, 1988), (ii) unability of grains to rotate (e.g., biotite inclusions in early-grown crystals, biotite flakes stuck in a crystal-rich framework), (iii) sequential overprinting of different processes. If more than one process affects the orientation of minerals in schlieren, we stress that the fabric could potentially serve as an indicator of finite strain associated with various processes of schlieren formation.

6.1. Interpretation of the measured EBSD patterns

Compared to the idealized schlieren fabric characteristics depicted in Fig. 11, the EBSD analysis of biotite schlieren in the Jizera granite reveals much more complex lattice-preferred orientations of biotite in all analyzed samples. Our interpretations of gradients in and geometry of internal schlieren fabric, as presented below, are based on the overall geometry of the schlieren-bearing structures, measured EBSD patterns, and changes of the lattice-preferred orientation of biotite with distance from the base of the schlieren. Despite the multimodal orientation distribution and a wide scatter of biotite crystallographic axes in some samples (e.g., Figs. 5c, f, i, 7a), the following three principal types of biotite fabric in the schlieren can be defined on the basis of the EBSD patterns.

(1) In Structure 1, the biotite basal planes (001), the pole of which is the *c* axis, exhibit two principal orientations within the same sample (Figs. 5f, 6c, f). Near the base of the schlieren, biotite basal planes tend to have schlieren-subparallel orientations (*c* axes maxima plot close to the schlieren pole; Figs. 5f, 6f, 7f), whereas in the upper part of the schlieren, biotite tends to reorient into a schlieren-perpendicular orientation (Figs. 5c, 6c, 7c). Regardless
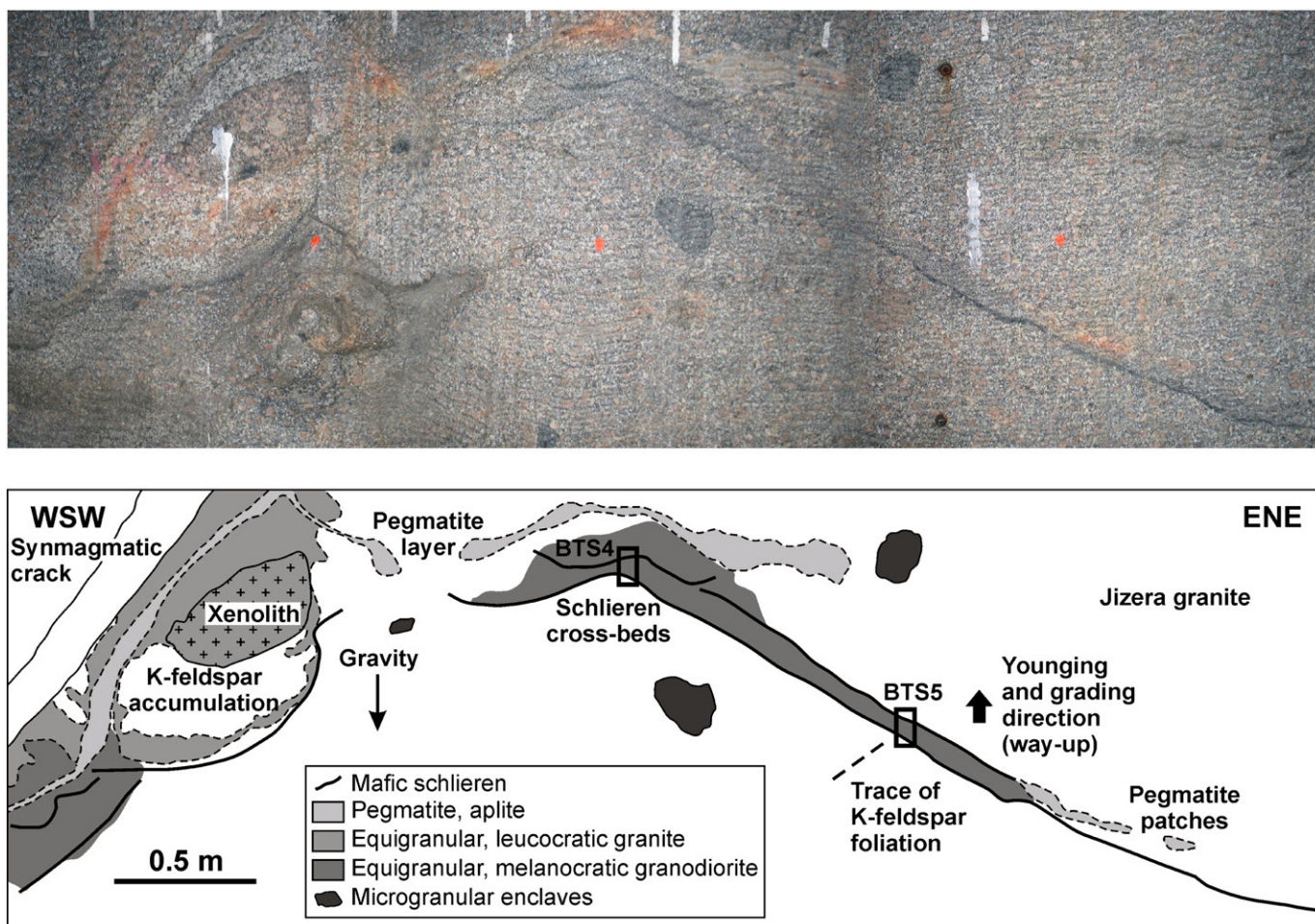
Fig. 8. Photomosaic and line drawing of a complex magmatic structure in the Jizera granite, Bedřichov tunnel, section A, approximately 210 m from the western entrance. The structure comprises a schlieren anticline (younging and grading upwards) with an overlying folded pegmatite layer. One limb of the schlieren anticline (on the right-hand side) is straight; the other limb is molded around the overlying K-feldspar accumulation (left-hand side). The xenolith rests on the top of the K-feldspar accumulation and does not disrupt the overlying pegmatite layer. A submagmatic crack with sharp outer margins and filled by the Jizera granite truncates the schlieren anticline. Bold rectangles indicate sample locations.

of the distance from the schlieren base, both schlieren-parallel and schlieren-perpendicular orientations of biotite share sub-horizontal ~N–S to ~NNE–SSW *a* axes (Figs. 5a, d, 6a, d, 7d).

We propose that such an orientation distribution of biotite crystallographic axes could be explained in terms of a velocity-gradient resulting from laminar flow along a rheological boundary (Fig. 12a). Near the base of the schlieren, greater shear strain presumably caused biotite alignment subparallel to the rigid wall, represented by the underlying high-viscosity granite magma mush. This high-shear-strain zone passes upwards into a zone where biotite is oriented nearly perpendicular to the schlieren. This gradual transition from schlieren-parallel to schlieren-perpendicular orientations of biotite is best documented in sample BTS2 (Fig. 6c, f).

As the *a* axes retain their orientation across these two zones, they seem to be aligned perpendicular to the flow velocity-gradient, that is, also to the bulk flow direction (Fig. 12a; the case of divergent flow of Paterson et al., 1998). This alignment was perhaps favored by the crystals' elongation in the *a* axes (Fig. 2c). Furthermore, the consistent positions of some *c* axes maxima with respect to the base of the schlieren define the fabric asymmetry (e.g., Blumenfeld and Bouchez, 1988) and allow inference of the bulk flow kinematics (Fig. 12a).

(2) In Structure 2, the measured EBSD patterns differ from those described above. Common, generalized features characterizing

both samples BTS4 and BTS5 are as follows. (i) The *a* axes are steep, at a high angle to the schlieren plane (their maxima plot near the centre of the stereonet; Fig. 9a, d, g), or tend to concentrate along the ~NE–SW plane lying both close to and at a high angle to the schlieren (girdles in Fig. 10a, d). (ii) The *c* axes plunge shallowly to moderately and define circular patterns parallel to the periphery of the stereonets (outside the *a* axes; Fig. 9c, f, i). (iii) The EBSD patterns are similar regardless of the position of the analyzed domain within the schlieren and, importantly, are also similar to that of the underlying granite (Fig. 9g–i).

We interpret the steeply-plunging *a* axes and their elongated girdles and shallowly plunging *c* axes near the periphery of the stereonets as a result of constrictional deformation where the *b* and *c* axes rotated around an ill-defined *a* axis (Fig. 12b). If so, the schlieren experienced a minor amount of stretching after their formation, sufficient to reorient biotite crystals but still retaining continuity of the schlieren and not destroying their original shapes. The orientation of the *a* axes indicates that the principal stretching direction was steep and oriented at a high angle to the schlieren plane; the *a* axis girdles (Fig. 12b) may be interpreted as recording various stages of the rotation of biotite crystals from the schlieren-subparallel orientation (*a* axes within the schlieren plane, *c* axes close to the schlieren pole) into a new, steep orientation. This process thus could not be related to the magma flow associated with the schlieren formation (compare to

Sample BTS4 - upper part of schlieren, ~2 cm from base
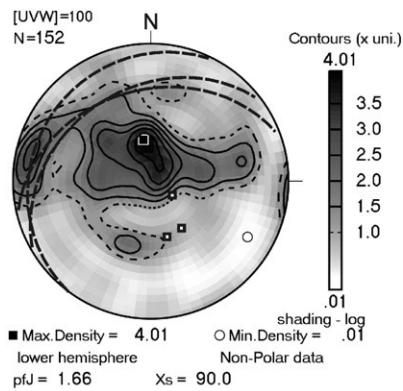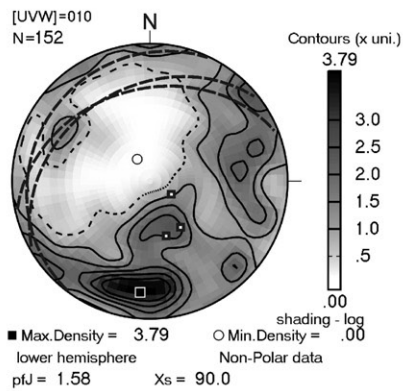
(a) *a* axes   **(b)** *b* axes   **(c)** *c* axes
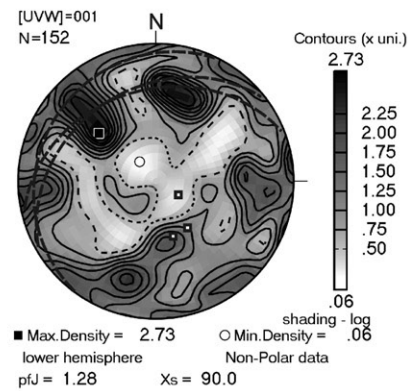
Sample BTS4 - base of schlieren
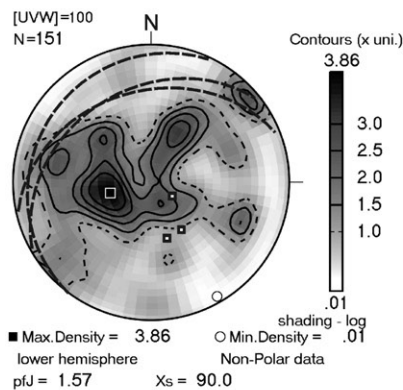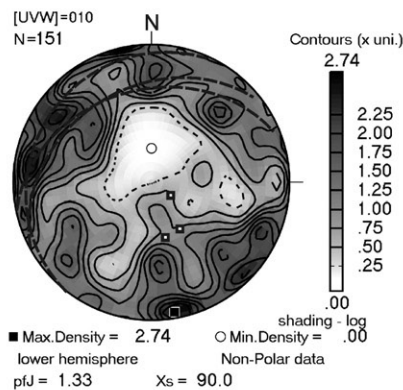
(d) *a* axes   **(e)** *b* axes   **(f)** *c* axes
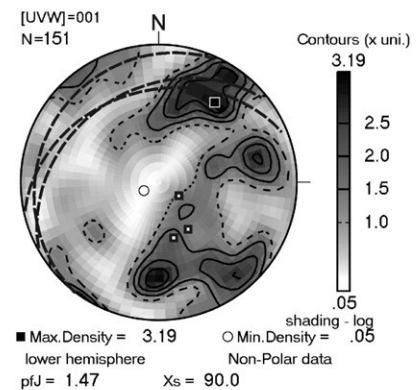
Sample BTS4 - granite beneath schlieren

(g) *a* axes   **(h)** *b* axes   **(i)** *c* axes
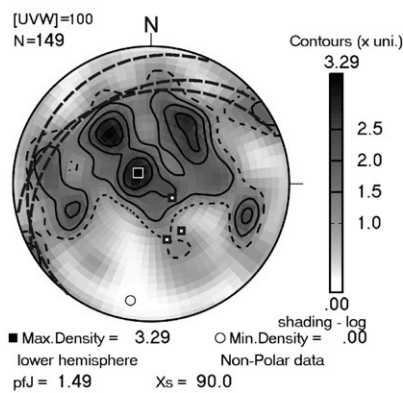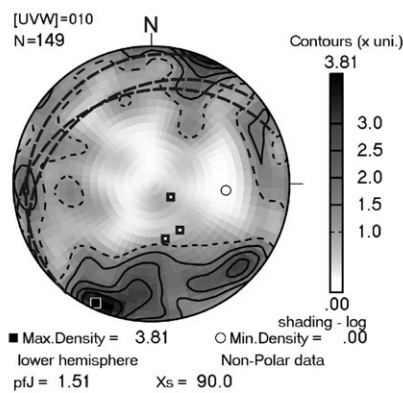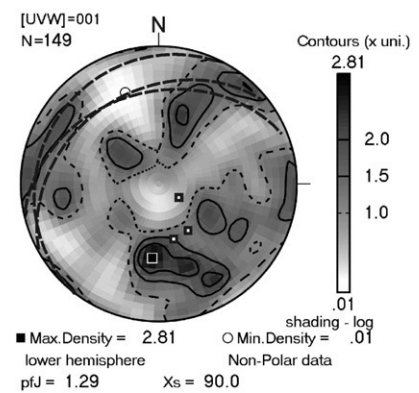
Great circle (dashed) - schlieren plane ▫ Pole to the schlieren plane

Fig. 9. Stereographic projection (equal area, lower hemisphere) of orientations of biotite crystallographic axes (*a, b, c*) in sample BTS4 (Structure 2) obtained using the EBSD method. The analysis was carried out in the host granite beneath the schlieren and in two domains at various distances from the base of the schlieren. See Fig. 8 for sample location. Orientations are shown in the geographic coordinate system.

fabric in Structure 1), nor to the background finite strain recorded by the host granite (Section 3, Fig. 3b, c). At a larger scale, the entire Structure 2 shows evidence for vertical magma movements; the exotic

granite xenolith obviously sank into the down-warped K-feldspar phenocryst accumulation and the central part of the anticline may have formed by the rise of the underlying granite mush (Fig. 8).

Sample BTS5 - upper part of schlieren, ~4.5 cm from base

(a) *a* axes   **(b)** *b* axes   **(c)** *c* axes
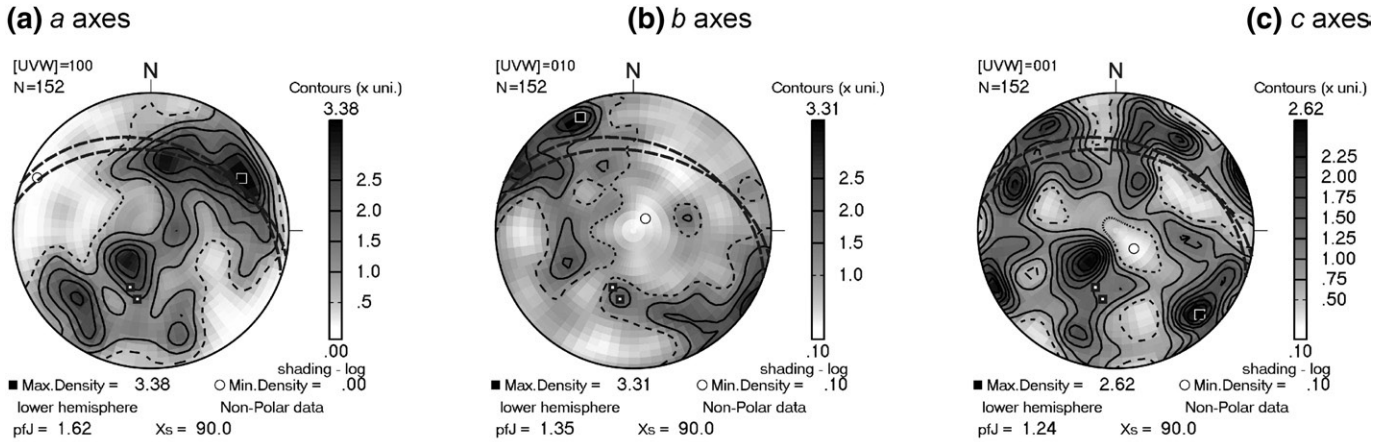
Sample BTS5 - base of schlieren

(d) *a* axes   **(e)** *b* axes   **(f)** *c* axes
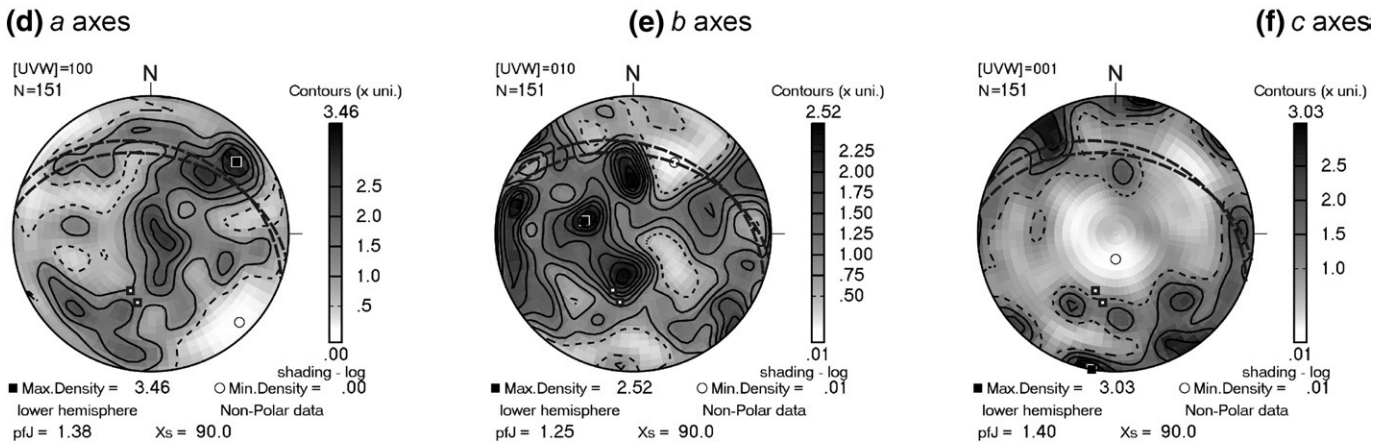
Great circle (dashed) - schlieren plane   ▫ Pole to the schlieren plane

Fig. 10. Stereographic projection (equal area, lower hemisphere) of orientations of biotite crystallographic axes (*a*, *b*, *c*) in sample BTS5 (Structure 2) obtained using the EBSD method. The analysis was carried out in two domains at various distances from the base of schlieren. See Fig. 8 for sample location. Orientations are shown in the geographic coordinate system.

Despite unknown kinematics (up or down), the biotite lattice-preferred orientation in the schlieren may also be viewed as a micro-scale manifestation of the same gravity-driven late adjustments of the magma mush, causing minor vertical stretching both in the schlieren and in the host granite prior to complete locking-up of the crystal framework.

(3) By contrast, in two domains of Structure 1, the *a* axes plunge shallowly to the SE or NW (most pronounced *a* axes maxima in Figs. 5g, 7a, respectively) while the *c* axes are subhorizontal and cluster around a ~NE–SW trend (Figs. 5i, 7c). The EBSD in these domains within the schlieren thus correspond well with the background magnetic (AMS) fabric of the host granite (Section 3; Fig. 3b, c with Figs. 5g, i, 7a, c). We interpreted elsewhere that the homogeneous orientation of AMS in the Jizera granite, carried by coaxial contributions of biotite, magnetite, and maghemite, reflects late hypersolidus (tectonic?) strain superimposed onto an earlier K-feldspar phenocryst fabric (Žák et al., 2008). This overprinting strain could account for the biotite lattice-preferred orientations being nearly perpendicular to the inferred flow

fabric and parallel to the background AMS principal directions in a few small domains within the schlieren.

6.2. Grain-scale processes during biotite fabric formation in schlieren

The multiple lattice-preferred orientations of biotite grains documented within a single schlieren structure indicate that the magma inside and around the schlieren was capable of actively deforming and recording minor increments of superposed strains without macroscopic distortion of the original schlieren shapes. If this is true, important questions emerge: by which micro-scale mechanism(s) were the multiple orientations of the biotite acquired, and what was the rheological state of the magma during the schlieren and biotite fabric formation?

Our interpretation is that the biotite schlieren in the Jizera granite formed by flow sorting coupled with interstitial melt extraction (e.g., Weinberg et al., 2001) along margins of magma flowing through localized channel-like domains (Žák and Klomínský, 2007). To preserve the schlieren and protect them from being destroyed by movements of the host magma, the channels delineated by the schlieren must have formed in an environment of relatively static (not flowing), high-

Physical process of schlieren formation	Strain state	Geometric characteristics of biotite shape-fabric	Expected EBSD pattern of biotite crystallographic axes
Gravitational settling under static or quasi-static conditions — Gravity; Overlying low-viscosity magma; Mafic schlieren; Underlying crystal mush	Rotation followed by uniaxial contraction perpendicular to schlieren	Modal grading: crystal spacing increases and shape-preferred orientation decreases from the base of schlieren. Basal planes of biotite statistically aligned parallel to the base of schlieren	c axes cluster; a axes girdle; Schlieren plane
Compaction coupled with melt extraction — Melt extraction; Porous crystal mush; Compaction zone (mafic schlieren); Porous crystal mush; Melt extraction	Uniaxial contraction perpendicular to schlieren	Basal planes of biotite statistically aligned parallel to schlieren plane	c axes cluster; a axes girdle; Schlieren plane
Velocity gradient flow along rheological boundary — Magma flow; Overlying low-viscosity magma; Mafic schlieren; Underlying crystal mush	Simple shear, schlieren-parallel shear plane	Crystal spacing increases from the base of schlieren. The angle between basal planes of biotite and schlieren plane increases away from schlieren	c axes; a-b plane; Schlieren plane; c axes
Late synmagmatic tectonic deformation — Principal shortening direction; Crystal mush; Mafic schlieren; Crystal mush	Overprinting regional contraction at an angle to the schlieren plane	Basal planes of biotite crystals aligned both parallel to schlieren and perpendicular to the overprinting principal shortening direction	c axes clusters; a axes girdles
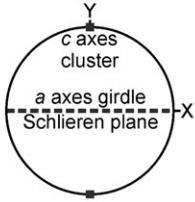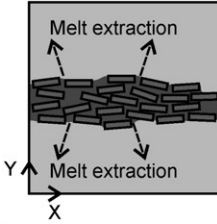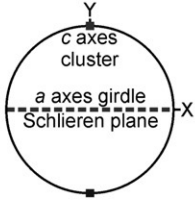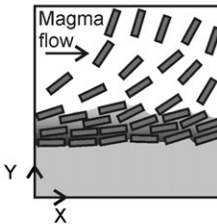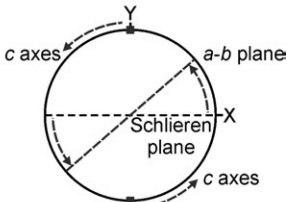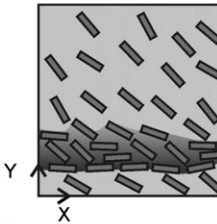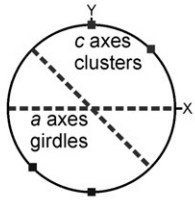
Fig. 11. Conceptual, simplified cartoon to summarize the main mechanical processes of schlieren formation, associated strain and fabric characteristics, and expected EBSD patterns of biotite crystallographic axes.

strength crystal-rich mush. We assume that the interlocked K-feldspar phenocrysts, which are up to 5 cm in size in the host Jizera granite, established a rigid, porous framework (similar to the Load Bearing Framework texture of Handy, 1994), and that the weaker channel-shaped regions within this framework were re-intruded by more mobile magma. During magma flow through these channels, biotite flakes inside the schlieren rotated to reflect the local flow geometry and kinematics (Fig. 12a).

After the localized flow in the channels had ceased, some biotite grains within the schlieren still could variably reorient in response to later strain increments, presumably by a mechanism of melt-aided grain-boundary sliding (GBS; e.g., Park and Means, 1996; Launeau and Cruden, 1998; Paterson et al., 1998, 2003; Rosenberg, 2001; Rosenberg and Handy, 2005). We envision that by this mechanism, biotite grains in small interstitial melt pockets within the otherwise locked-up cumulate could record some other processes that postdated schlieren formation and were superimposed onto the magma mush prior to its full crystallization. In the case of the Jizera granite, such late processes may have been gravity-driven grain-scale constrictional deformation of the mush (at a high angle to the schlieren), or may be related to differential (tectonic?) stresses transmitted across the crystallizing magma chamber, such as the deformation recorded by the background AMS fabric in the host granite.

These inferences are in agreement with recent studies on granite rheology and melt topology in partially molten granites (Rosenberg and Handy, 2005) that suggest that 90% of crystal boundaries are lubricated by melt even at less than 10% melt volume in the system. Thus, the earlier flow-related fabric(s) may have been heterogeneously overprinted even at the high magma crystallinities required to preserve the schlieren. The heterogeneous nature of fabric superposition in the schlieren is further evidenced by (1) the multiple orientations of biotite crystallographic axes, which are either random or may be assigned to various types of fabric and are measured in a single sample of schlieren, and by (2) the gradual transitions from flow-related to the late-strain-related fabric, the latter also being recorded by the surrounding granite.
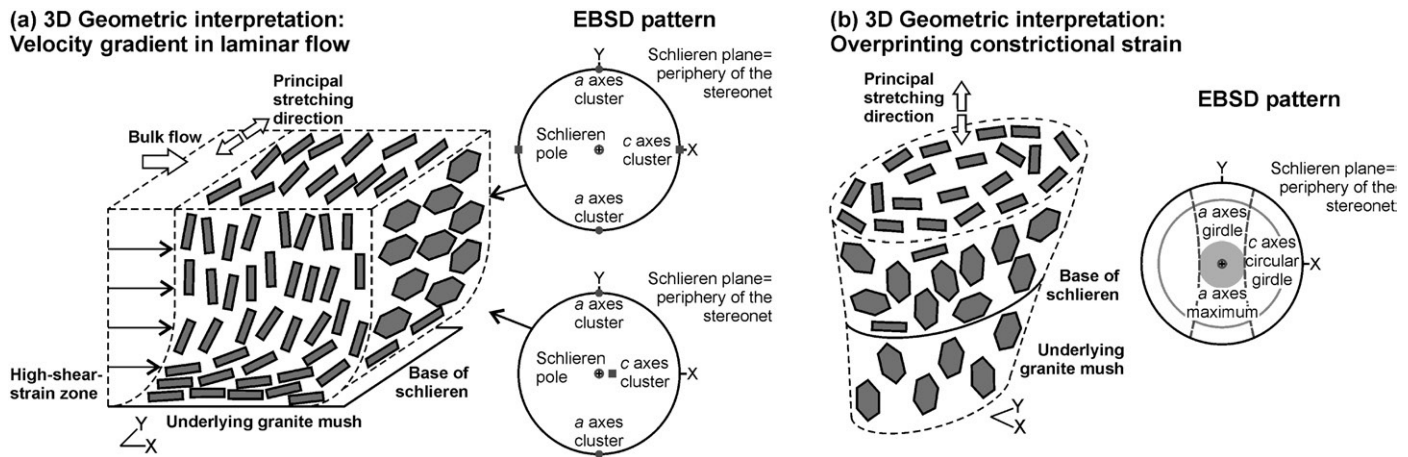
Fig. 12. (a, b) Simplified three-dimensional geometric interpretation of the measured EBSD patterns from Structures 1 and 2, respectively. The orientations of biotite *a* and *b* axes are shown with respect to the schlieren plane (horizontal, *X–Y*) and projected onto the lower hemisphere (stereonets). (a) In Structure 1, the orientation of biotite crystals is interpreted as being a result of schlieren-parallel laminar magma flow, with the principal stretching oriented perpendicular to the bulk flow direction. (b) In Structure 2, *a* axes are predominantly oriented at a high angle to the schlieren plane as a result of constrictional deformation of the magma mush; the vertical stretching likely postdates the schlieren formation.

We interpret the above to indicate that, in a single small volume of the schlieren (size of the EBSD sample), some biotite grains were mechanically locked up in random orientations presumably adjusted to irregular grain boundaries in the crystal mush, giving rise to random, scattered orientations of some crystallographic axes in the stereonets (e.g., Fig. 5c, f, i). Some grains were realigned during velocity-gradient flow (Fig. 12a), whereas other melt-lubricated grains were finally reoriented by the grain-boundary sliding in response to the late deformation of a stiff mush. As suggested by the "poikilitic-type" schlieren microstructure (Fig. 2), biotite crystals were trapped at various stages of reorientation by increasingly viscous interstitial melt and rapidly overgrown by the K-feldspar and quartz matrix.

7. Conclusions

The multiple lattice-preferred orientations of biotite in mafic schlieren hosted in the Jizera granite are interpreted to reflect (1) localized laminar magma flow along channel-like conduits within the high-strength host phenocryst framework, (2) grain-scale gravity-driven constrictional deformation of the magma mush, and (3) overprinting background deformation transmitted across large parts of the magma chamber prior its final crystallization.

At the grain-scale, the main mechanisms of biotite fabric acquisition in the schlieren may have involved rotation of biotite crystals during velocity-gradient channel flow, with the biotite alignment reflecting the magma flow geometry and kinematics. After the flow cessation, the rotation was replaced by melt-aided grain-boundary sliding of those biotite crystals that were still embedded in melt pockets within otherwise static, highly crystallized magma mush. The latter process was sufficient to reorient biotite grains but not to cause destruction of the schlieren-bearing structures.

Using the Jizera granite as a case example, we argue that the lattice-preferred orientation of mineral grains in mafic schlieren is highly sensitive to capturing strain accumulated in crystal-rich mushes and resulting from a variety of mechanical processes. The cumulate mineral grains in the schlieren may sequentially reorient in response to processes both associated with the schlieren formation (e.g., localized magma flow) and those that occur later, which are superimposed onto the effectively solid, high-strength magma mush.

In conclusion, the EBSD method has proven particularly useful to reveal flow geometry and kinematics during schlieren formation. In combination with other techniques (field mapping, AMS, computer-aided image analysis), the EBSD may help to unravel progressive strain histories of ancient magma chambers from an earlier strain recorded in the host phenocryst framework (e.g., Žák et al., 2008) through local strain in mafic schlieren (this study) to late overprinting strain in the inter-phenocryst matrix detected using AMS (e.g., this study; Žák et al., 2008, in press).

References

Aleksandrowski, P., Mazur, S., 2002. Collage tectonics in the northeasternmost part of the Variscan Belt: the Sudetes, Bohemian Massif. In: Winchester, J.A., Pharaoh, T.C., Verniers, J. (Eds.), Palaeozoic Amalgamation of Central Europe. Geological Society, London, Special Publications, vol. 201, pp. 237–277.

Aleksandrowski, P., Kryza, R., Mazur, S., Zaba, J., 1997. Kinematic data on major Variscan strike–slip faults and shear zones in the Polish Sudetes, northeast Bohemian Massif. Geological Magazine 134 (5), 727–739.

Aleksandrowski, P., Kryza, R., Mazur, S., Pin, C., Zalasiewicz, J.A., 2000. The Polish Sudetes: Caledonian or Variscan? Transactions of the Royal Society of Edinburgh. Earth Sciences 90 (2), 127–146.

Barbey, P., Gasquet, D., Pin, C., Bourgeix, A.L., 2008. Igneous banding, schlieren and mafic enclaves in calc-alkaline granites: the Budduso pluton (Sardinia). Lithos 104 (1–4), 147–163.

Barriére, M., 1981. On curved laminae, graded layers, convection currents and dynamic crystal sorting in the Ploumanac'h (Brittany) subalkaline granite. Contributions to Mineralogy and Petrology 77 (3), 214–224.

Blumenfeld, P., Bouchez, J.L., 1988. Shear criteria in granite and migmatite deformed in the magmatic and solid states. Journal of Structural Geology 10 (4), 361–372.

Bonlen, S.R., Peacor, D.R., Essene, E.J., 1980. Crystal chemistry of a metamorphic biotite and its significance in water barometry. American Mineralogist 65 (1–2), 55–62.

Borkowska, M., 1966. Petrography of Karkonosze granite. Geologia Sudetica 2, 7–119.

Borradaile, G., 2003. Statistics of Earth Science data: their distribution in space, time, and orientation. Springer, Berlin. 351 pp.

Bouchez, J.L., 1997. Granite is never isotropic: an introduction to AMS studies of granitic rocks. In: Bouchez, J.L., Hutton, D.H.W., Stephens, W.E. (Eds.), Granite: from Segregation of Melt to Emplacement Fabrics. Kluwer Academic Publishers, pp. 95–112.

Clarke, D.B., Clarke, G.K.C., 1998. Layered granodiorites at Chebucto Head, South Mountain batholith, Nova Scotia. Journal of Structural Geology 20 (9–10), 1305–1324.

Cloos, H., 1925. Einführung in die tektonische Behandlung magmatischer Erscheinungen (Granittektonik). 1. Das Riesengebirge in Schlesien. Borntraeger, Berlin, p. 194.

Cymerman, Z., Piasecki, M.A.J., Seston, R., 1997. Terranes and terrane boundaries in the Sudetes, northeast Bohemian Massif. Geological Magazine 134 (5), 717–725.

Duthou, J.L., Couturie, J., Mierzejewski, M., Pin, C., 1991. Dating a granite sample from the Karkonosze Mountains using the Rb/Sr whole rock isochron method. Przeglad Geologiczny 39 (2), 75–78.

Fliervoet, T.F., Drury, M.R., Chopra, P.N., 1999. Crystallographic preferred orientations and misorientations in some olivine rocks deformed by diffusion or dislocation creep. Tectonophysics 303 (1–4), 1–27.

Handy, M.R., 1994. Flow laws for rocks containing two non-linear viscous phases: a phenomenological approach. Journal of Structural Geology 16 (3), 287–301.

Heidelbach, F., Kunze, K., Wenk, H-R., 2000. Texture analysis of a recrystallized quartzite using electron diffraction in the scanning electron microscope. Journal of Structural Geology 22 (1), 92–101.

Hladil, J., Patočka, F., Kachlík, V., Melichar, R., Hubačík, M., 2003. Metamorphosed carbonates of Krkonoše Mountains and Paleozoic evolution of Sudetic terranes (NE Bohemia, Czech Republic). Geologica Carpathica 54 (5), 291–297.

Holness, M.B., 2007. Textural immaturity of cumulates as an indicator of magma chamber processes: infiltration and crystal accumulation in the Rum Eastern Layered Intrusion. Journal of the Geological Society, London 164 (3), 529–539.

Hrouda, F., 1982. Magnetic anisotropy of rocks and its application in geology and geophysics. Geophysical Surveys 5 (1), 37–82.

Klomínský, J., 1969. The Krkonoše–Jizera granitoid massif. Sborník geologických věd 15, 1–134.

Klomínský, J. (Ed.), 2005. Geological and Structural Characterization of Granitoids in Water-plant Tunnels in the Jizera Mountains. Final report, Radioactive Waste Repository Authority (SÚRAO), Prague. 159 pp.

Kozdrój, W., Krentz, O., Opletal, M. (Eds.), 2001. Geological Map Lausitz-Jizera-Karkonosze (without Cenozoic sediments), 1:100,000. Sächsisches Landesamt für Umwelt und Geologie, Panstwowy Instytut Geologiczny. Česká geologická služba, Warszaw.

Kröner, A., Hegner, E., Hammer, J., Haase, G., Bielicki, K.H., Krauss, M., Eidam, J., 1994. Geochronology and Nd–Sr systematics of Lusatian granitoids — significance for the evolution of the Variscan orogen in East-Central-Europe. Geologische Rundschau 83 (2), 357–376.

Launeau, P., Cruden, A.R., 1998. Magmatic fabric acquisition in a syenite: results of a combined anisotropy of magnetic susceptibility and image analysis study. Journal of Geophysical Research 103 (B3), 5067–5089.

Leiss, B., Barber, D.J., 1999. Mechanisms of dynamic recrystallization in naturally deformed dolomite inferred from EBSP analyses. Tectonophysics 303 (1–4), 51–69.

Lloyd, G.E., Freeman, B., 1994. Dynamic recrystallization of quartz under greenschist conditions. Journal of Structural Geology 16 (6), 867–881.

Machowiak, K., Armstrong, R., 2007. SHRIMP U–Pb zircon age from the Karkonosze granite. Mineralogia Polonica Special Papers 31, 193–196.

Marheine, D., Kachlík, V., Maluski, H., Patočka, F., Zelazniewicz, A., 2002. The ^{40}Ar/^{39}Ar ages from the West Sudetes (NE Bohemian Massif): constraints on the Variscan tectonothermal development. In: Winchester, J.A., Pharaoh, T.C., Verniers, J. (Eds.), Palaeozoic Amalgamation of Central Europe. Geological Society, 201. Special Publications, London, pp. 133–155.

Mazur, S., 2002. Geology of the Karkonosze–Izera Massif: an overview. Mineralogical Society of Poland, Special Papers 20, 22–34.

Mazur, S., Aleksandrowski, P., 2001. The Teplá(?)/Saxothuringian suture in the Karkonosze–Izera massif, western Sudetes, central European Variscides. International Journal of Earth Sciences 90 (2), 341–360.

Mazur, S., Aleksandrowski, P., Kryza, R., Oberc-Dziedzic, T., 2006. The Variscan orogen in Poland. Geological Quarterly 50 (1), 89–118.

McLaren, S., Reddy, S.M., in press. Automated mapping of K-feldspar by electron backscatter diffraction and application to 40Ar/39Ar dating. Journal of Structural Geology. doi:10.1016/j.jsg.2008.05.008.

Milord, I., Sawyer, E.W., 2003. Schlieren formation in diatexite migmatite: examples from the St Malo migmatite terrane, France. Journal of Metamorphic Geology 21 (4), 347–362.

Mitchell, A.A., Eales, H.V., Krueger, F.J., 1998. Magma replenishment and the significance of poikilitic textures in the Lower Main Zone of the western Bushveld Complex, South Africa. Mineralogical Magazine 62 (4), 435–450.

Naney, M.T., Swanson, S.E., 1980. The effect of Fe and Mg on crystallization in granitic systems. American Mineralogist 65 (7–8), 639–653.

Prior, D.J., Boyle, A.P., Brenker, F., Cheadle, M.C., Day, A., Lopez, G., Peruzzo, L., Potts, G.J., Reddy, S., Spiess, R., Timms, N.E., Trimby, P., Wheeler, J., Zetterström, L., 1999. The application of electron backscatter diffraction and orientation contrast imaging in the SEM to textural problems in rocks. American Mineralogist 84 (11–12), 1741–1759.

Park, Y., Means, W.D., 1996. Direct observation of deformation processes in crystal mushes. Journal of Structural Geology 18 (6), 847–858.

Paterson, S.R., Vernon, R.H., Tobisch, O.T., 1989. A review of criteria for identification of magmatic and tectonic foliations in granitoids. Journal of Structural Geology 11 (3), 349–363.

Paterson, S.R., Fowler, T.K., Schmidt, K.L., Yoshinobu, A.S., Yuan, E.S., Miller, R.B., 1998. Interpreting magmatic fabric patterns in plutons. Lithos 44 (1–2), 53–82.

Paterson, S.R., Onezime, J., Teruya, L., Žák, J., 2003. Quadruple-pronged enclaves: their significance for the interpretation of multiple magmatic fabrics in plutons. Journal of the Virtual Explorer 10, Electronic Edition, General Contributions 2005, 15–30.

Pons, J., Barbey, P., Nachit, H., Burg, J.P., 2006. Development of igneous layering during growth of pluton: the Tarcouate Laccolith (Morocco). Tectonophysics 413 (3–4), 271–286.

Pupier, E., Barbey, P., Toplis, M.J., Bussy, F., 2008. Igneous layering, fractional crystallization and growth of granitic plutons: the Dolbel batholith in SW Niger. Journal of Petrology 49 (6), 1043–1068.

Romeo, I., Capote, R., Lunar, R., Cayzer, N., 2007. Polymineralic orientation analysis of magmatic rocks using electron back-scatter diffraction: implications for igneous fabric origin and evolution. Tectonophysics 444 (1–4), 45–62.

Rosenberg, C.L., 2001. Deformation of partially molten granite: a review and comparison of experimental and natural case studies. International Journal of Earth Sciences 90 (1), 60–76.

Rosenberg, C.L., Handy, M.R., 2005. Experimental deformation of partially melted granite revisited: implications for the continental crust. Journal of Metamorphic Geology 23 (1), 19–28.

Schmidt, N.H., Olesen, N.O., 1989. Computer-aided determination of crystal-lattice orientation from electron-channelling patterns in the SEM. Canadian Mineralogist 27 (1), 15–22.

Słaby, E., Götze, J., 2004. Feldspar crystallization under magma-mixing conditions shown by cathodoluminescence and geochemical modelling — a case study from the Karkonosze pluton (SW Poland). Mineralogical Magazine 68 (4), 561–577.

Słaby, E., Martin, H., 2008. Mafic and felsic magma interaction in granites: the Hercynian Karkonosze pluton (Sudetes, Bohemian Massif). Journal of Petrology 49 (2), 353–391.

Słaby, E., Galbarczyk-Gasiorowska, L., Baskiewicz, A., 2002. Mantled alkali-feldspar megacrysts from the marginal part of the Karkonosze granitoid massif (SW Poland). Acta Geologica Polonica 52 (4), 501–519.

Słaby, E., Galbarczyk-Gasiorowska, L., Seltmann, R., Müller, A., 2007a. Alkali feldspar megacryst growth: geochemical modelling. Mineralogy and Petrology 89, 1–29.

Słaby, E., Seltmann, R., Kober, B., Müller, A., Galbarczyk-Gasiorowska, L., Jeffries, T., 2007b. LREE distribution patterns in zoned alkali feldspar megacrysts from the Karkonosze pluton, Bohemian Massif — implications for parental magma composition. Mineralogical Magazine 71, 193–217.

Tarling, D.H., Hrouda, F., 1993. The Magnetic Anisotropy of Rocks. Chapman and Hall, London, p. 217.

Vernon, R.H., 2000. Review of microstructural evidence of magmatic and solid-state flow. Electronic Geosciences 5 (2), 1–23.

Verner, K., Žák, J., Hrouda, F., Holub, F., 2006. Magma emplacement during exhumation of the lower- to mid-crustal orogenic root: the Jihlava syenitoid pluton, Moldanubian Unit, Bohemian Massif. Journal of Structural Geology 28 (8), 1553–1567.

Weinberg, R.F., Sial, A.N., Pessoa, R.R., 2001. Magma flow within the Tavares pluton, northeastern Brazil: compositional and thermal convection. Geological Society of America Bulletin 113 (4), 508–520.

Wiebe, R.A., Jellinek, M., Markley, M.J., Hawkins, D.P., Snyder, D., 2007. Steep schlieren and associated enclaves in the Vinalhaven granite, Maine: possible indicators for granite rheology. Contributions to Mineralogy and Petrology 153 (4), 121–138.

Winchester, J.A., Patočka, F., Kachlík, V., Melzer, M., Nawakowski, C., Crowley, Q.G., Floyd, P.A., 2003. Geochemical discrimination of metasedimentary sequences in the Krkonoše-Jizera terrane (west Sudetes, Bohemian Massif): paleotectonic and stratigraphic constraints. Geologica Carpathica 54 (5), 267–280.

Žák, J., Klomínský, J., 2007. Magmatic structures in the Krkonoše–Jizera Plutonic Complex, Bohemian Massif: evidence for localized multiphase flow and small-scale thermal–mechanical instabilities in a granitic magma chamber. Journal of Volcanology and Geothermal Research 164 (4), 254–267.

Žák, J., Verner, K., Týcová, P., 2008. Multiple magmatic fabrics in plutons: an overlooked tool for exploring interactions between magmatic processes and regional deformation? Geological Magazine 145 (4), 1–15.

Žák, J., Verner, K., Klomínský, J., Chlupáčová, M., in press. "Granite tectonics" revisited: insights from comparison of K-feldspar shape-fabric, anisotropy of magnetic susceptibility (AMS), and brittle fractures in the Jizera granite, Bohemian Massif. International Journal of Earth Sciences. doi:10.1007/s00531-007-0292-x.

Zelazniewicz, A., 1997. The Sudetes as a Palaeozoic orogen in central Europe. Geological Magazine 134 (5), 691–702.